Electron paramagnetic resonance of heterogeneous chromium catalysts

Bert M. Weckhuysen,[a]*† Robert A. Schoonheydt,[a] Frank E. Mabbs[b] and David Collison[b]
[a] *Centrum voor Oppervlaktechemie en Katalyse, K.U.Leuven, Kardinaal Mercierlaan 92, 3001 Heverlee, Belgium*
[b] *Department of Chemistry, University of Manchester, Manchester, UK M13 9PL*

The X- and Q-band EPR spectra of Cr^{5+} and Cr^{3+} ions in heterogeneous Cr catalysts have been investigated as a function of the support type and composition (silica, silica–alumina, alumina, mordenite and AlPO-5). A spin-Hamiltonian operator for each of the observed types of resonances is proposed and discussed, while the extensive use of computer-simulated spectra provides detailed information on the nature of supported Cr ions. Mononuclear Cr^{5+} ions (γ-signal), with g-values *ca.* 2, are axial on alumina and silica–alumina, and rhombic on silica and mordenite. Two different X-band EPR signals of Cr^{3+} ions are present on amorphous and crystalline oxidic surfaces: a broad signal with g around 2 and zero field parameters D and E equal to 0, due to clustered Cr^{3+} (β-signal) or isolated octahedral Cr^{3+} complexes, and a signal with a positive lobe in the region $g = 3.5$–5.5 (δ-signal). The latter signal is characterized by high values of D and E and due to the presence of a highly distorted Cr^{3+} octahedron. The data so obtained allow us to develop a general model of supported Cr^{5+} and Cr^{3+} ions on oxidic surfaces.

Heterogeneous chromium catalysts are well known for their catalytic performances[1] and have been extensively studied in the past, especially the industrially used Phillips catalyst (Cr/SiO_2).[2] Cr^{3+} (d^3) and Cr^{5+} (d^1) are the EPR visible ions and therefore many characterization studies, based on electron paramagnetic resonance, have appeared in the literature.[3–11] The main literature results, mostly obtained from visual inspection of the experimental spectra, are summarized in Table 1.

On amorphous supports, three different signals, denoted as γ-, β- and δ-signal, are observed. Thus the axially symmetric Cr^{5+} signal (γ-signal), which has a sharp $g_\perp$ line and a weak somewhat diffuse $g_\parallel$ line, is assigned to a square pyramidal species in γ-alumina and a distorted tetrahedral species in silica, with both types of species proposed for Cr/zeolites. Recently, Cordischi *et al.*[12] re-investigated the Cr^{5+} signals on amorphous supports using X-band EPR after interaction with water and ammonia by using ^{53}Cr isotopes and simulation procedures. They showed that Cr^{5+} ions can be present on oxidic surfaces with (pseudo-) tetrahedral, square pyramidal and (pseudo-) octahedral coordination, depending on the treatment and on the support. Furthermore, they believed that the EPR spectra of Cr^{5+} on silica surfaces are slightly rhombic.

Cr_2O_3 cluster signals (β-signal) are strongly dependent on size and shape of these clusters as evidenced by the broad range of g-values. They have been especially evident for Cr/Al_2O_3 catalysts after reduction and recalcination.[13] Dispersed Cr^{3+} (δ-signal) is characterized by a broad signal around $g = 4.4$–5.0. It has only a positive lobe and overlaps with Fe^{3+} signals, making its assignment difficult and sometimes ambiguous. In general, its intensity increases with Cr loading and with reduction temperature and with these two parameters constant, with the alumina content of the support.[13]

Both the description of the signals and their interpretation have been vague in the literature. A more detailed picture of the EPR active, supported Cr is presented here. This is carried out taking spectra at X- and Q-band, and by a systematic simulation of the experimental spectra. The studied inorganic oxides are silica, alumina, silica–alumina, mordenite and AlPO-5, which allowed us to develop a more general model of supported Cr.

† E-mail address: Bert.Weckhuysen@agr.kuleuven.ac.be

Experimental

Preparation and treatment of samples

Cr/SiO_2, Cr/Al_2O_3 and $Cr/SiO_2 \cdot Al_2O_3$ (with 40 wt.% SiO_2) catalysts were prepared by the incipient wetness method with CrO_3 as impregnation salt using purpose-built supports. The preparation method and the characteristics of these supports are published elsewhere[14–16] and the Cr loading was 0.2 wt.%. A chromium exchanged mordenite zeolite (Cr/mordenite with unit cell composition: $Cr_{0.19}Na_{0.31}Al_{0.5}Si_{47.5}O_{96}$) and chromium substituted AlPO-5 molecular sieve (CrAPO-5 with unit cell composition: $Cr_{0.24}Al_{11.76}P_{12}O_{48}$) were prepared by methods fully described in previous papers.[17–19] The samples were dried at 50 °C for 8 h and then granulated. The size fraction 0.25–40 mm was loaded in a quartz flow cell with a side arm for EPR. The samples were subsequently dried at 90 °C for 16 h followed by calcination at 550 °C for 6 h in an oxygen stream. The quartz cell was purged with nitrogen and EPR spectra were recorded on these calcined samples. The samples were then reduced with CO between 200 and 600 °C in steps of 100 °C and EPR spectra were measured at each temperature. The O_2 and CO flows were, for all the pretreatments, 3600 and 1800 ml h^{-1}, respectively.

Electron paramagnetic resonance spectroscopy

EPR spectra of the samples were taken on a Bruker (Billeria, MA, USA) Model ESP300E instrument at the X-band between 120 and 370 K and a Varian (Palo Alto, CA, USA) E112 spectrometer at the Q-band and X-band at 300 K and 150 K. EPR simulations were performed by simulation programs developed by Mabbs and Collison and written in FORTRAN 4, processed with a FTN45 conversion package and using NAG library routines.[20,21]

Table 1 Literature survey of EPR parameters of Cr^{5+} and Cr^{3+} ions in heterogeneous chromium catalysts

heterogeneous Cr catalysts	EPR parameters	assignments	ref.
Cr/Al_2O_3	$g_{\|} = 1.955$; $g_{\perp} = 1.975$	γ-signal: Cr^{5+} ions in square pyramidal coordination	3–8
	$g_{eff} = 1.96$–2.45	β-signal: Cr_2O_3 clusters	
	positive lobe around $g_{eff} = 5.0$	δ-signal: dispersed Cr^{3+} ions	
Cr/SiO_2	$g_{\|} = 1.952$; $g_{\perp} = 1.972$	γ-signal: Cr^{5+} ions in square pyramidal coordination	
	$g_{\|} = 1.898$; $g_{\perp} = 1.975$	γ-signal: Cr^{5+} ions in distorted tetrahedral coordination	
	positive lobe around $g_{eff} = 4.4$	δ-signal: dispersed Cr^{3+} ions	
ion exchanged Cr/Y	$g_{eff} = 1.968$	$Cr^{3+}(H_2O)_x(Z{-}O^-)_y$ with Z = zeolite Y	9
calcined Cr/Y	$g_{\|} = 1.940$; $g_{\perp} = 1.987$	Y_1-signal: $[Cr{=}O]^{3+}$ ion at site II	10
	$g_{\|} = 1.915$; $g_{\perp} = 1.980$	Y_2-signal: $[Cr{=}O]^{3+}$ ion at site I' or II'	
calcined/mordenite	$g_{xx} = 1.9867$; $g_{yy} = 1.9720$; $g_{zz} = 1.9110$	A-signal: square pyramidal $[Cr{=}O]^{3+}$ ion in main channel	11
	$g_{\|} = 1.9947$; $g_{\perp} = 1.9070$	B-signal: distorted tetrahedral $[Cr{=}O]^{3+}$ ion at junction between main channel and the side pocket	

Superconducting quantum interference devices

Superconducting quantum interference devices (SQUID) measurements on Cr/SiO_2 and Cr/Al_2O_3 catalysts were carried out using apparatus from Oxford Instruments (Oxford, UK). The applied magnetic field was equal or below 1 T and the magnetic susceptibility (χ) was measured as a function of temperature (T) between 300 and 4.5 K. The samples were pretreated at 550 °C in oxygen in an EPR-DRS flow cell, followed by a vacuum treatment at room temperature. The EPR tubes were filled with 1 cm powder and sealed off under vacuum.

Results

Cr^{5+} signals

Cr^{5+} signals were observed after oxidative treatment and evacuation of molecular oxygen. Examples of the γ-signal are shown in Fig. 1 for Cr/Al_2O_3 and Cr/SiO_2 catalysts. The γ-signals of the $Cr/SiO_2 \cdot Al_2O_3$ were similar to those of Cr/Al_2O_3 and will not be shown. In some cases, the spectrum of Cr/SiO_2 comprises two different signals as evidenced in Fig. 2 by the weak $g_{\|}$ lines around 0.35 and 0.36 T. The g-values obtained by simulation with an axial/rhombic Hamiltonian are summarized in Table 2. The simulated spectra are also included in Fig. 1 and 2. For Cr^{5+} on alumina and silica–alumina, the g-values are axial with $g_{\|} = 1.910$–1.939 and $g_{\perp} = 1.975$–1.979, respectively. On silica, however, there are two distinct sets of signals one axial and the other clearly rhombic with $g_{xx} = 1.978$; $g_{yy} = 1.969$ and $g_{zz} = 1.895$. The latter signal is always dominant and its rhombic symmetry is in line with observations of Cordishi *et al.*[12] The shoulder on the low field side of the spectrum in Fig. 1B is weak and due to some axially symmetric Cr^{5+}. Its simulation, however, is not included in Fig. 1. The increase of the linewidth in going from silica to alumina is due to interaction of the unpaired electron of Cr^{5+} with ^{27}Al nuclei ($I = 5/2$) and may eventually obscure the rhombic symmetry on alumina. An example of a Q-band EPR spectra for Cr/Al_2O_3 is given in Fig. 3. This spectrum can be simulated by using the same parameters (except the linewidths) as for the X-band spectrum. The same holds for the Cr/SiO_2 and $Cr/SiO_2 \cdot Al_2O_3$ catalysts.

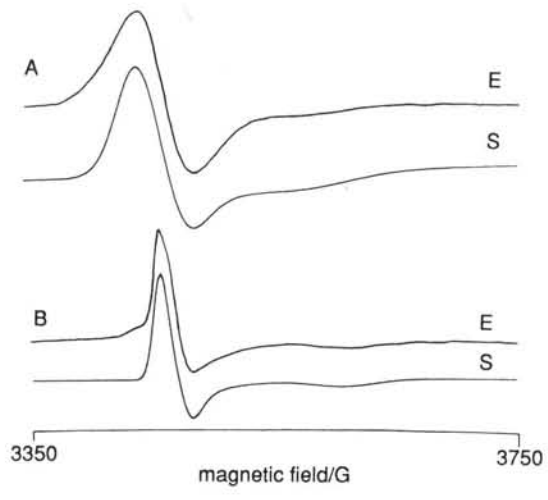

Fig. 1 Experimental (E) and simulated (S) X-band EPR spectra of Cr^{5+} on amorphous supports measured at 120 K: alumina (A) and silica (B)

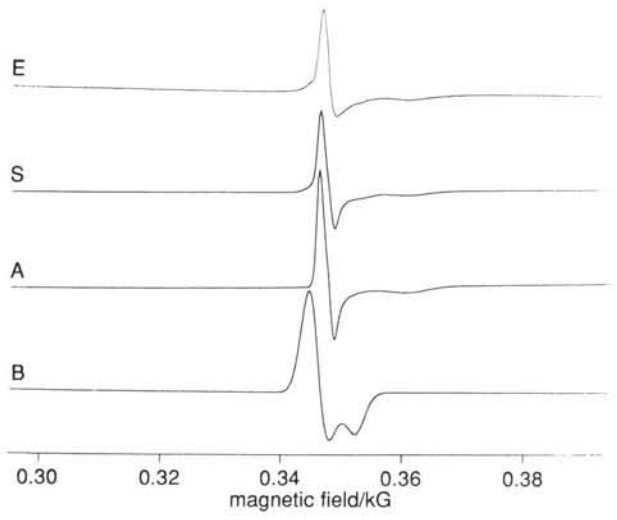

Fig. 2 Experimental X-band EPR spectrum measured at 120 K of 0.2 wt.% Cr/SiO_2 reduced at 200 °C (E), the simulated spectra of species A and B and the sum of the simulated spectra (S)

Table 2 EPR parameters for Cr^{5+} in various inorganic oxides obtained from fitting the experimental powder spectra

material	signal	g_{xx}	g_{yy}	g_{zz}	w_{xx}/G	w_{yy}/G	w_{zz}/G
Cr/Al_2O_3	A	1.978	1.978	1.910	45.0	45.0	70.0
$Cr/SiO_2 \cdot Al_2O_3$	A	1.975	1.975	1.910	50.0	50.0	65.0
Cr/SiO_2	A	1.979	1.979	1.939	30.0	30.0	30.0
	B	1.978	1.969	1.895	9.0	12.0	60.0
Cr/mordenite	C	2.000	1.980	1.920	18.0	14.0	20.0
	D	1.980 ($A_{xx(Al)} = 0.7$ mT)	1.990	1.930	25.0	5.0	25.0

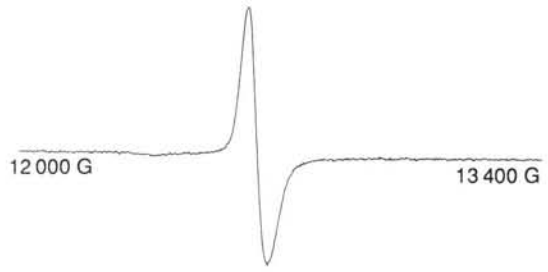

Fig. 3 Q-band EPR spectrum of Cr^{5+} on alumina measured at 150 K

The intensities of the γ-signal follow the the Curie-Weiss law and the χ^{-1} *vs.* T plots, obtained by SQUID measurements show a true paramagnetic behaviour down to 10 K. Between 10 and 4.5 K antiferromagnetic features were observed and consequently the χ^{-1} *vs.* T plots deviate from linearity. Only for Cr/SiO_2 was the diamagnetic contribution high and this made it impossible to measure reasonable χ^{-1} *vs.* T plots. In any case, our data show the presence of magnetically isolated Cr^{5+} species. This rejects also the earlier proposal for the γ-signal consisting of a trinuclear cluster (Cr^{3+}—Cr^{6+}—Cr^{3+})[22,23] because such clusters would not result in linear χ^{-1} *vs.* T plots. This conclusion is in line with earlier work of Cordishi *et al.*[12] and Cimino *et al.*[24]

The EPR spectrum of Cr^{5+} in mordenite molecular sieves, shown in Fig. 4, is very complex and can be described by two rhombic signals C and D. Signal D possesses a six-line superhyperfine splitting, indicative of close proximity between Cr and Al ($I = 5/2$). The simulated spectrum, together with the individual components C and D, are also shown in Fig. 4 and the overall simulated spectrum is very close to the experimental one. This analysis is different from that of Huang *et al.*[11] in that two rhombic signals are revealed by simulation.

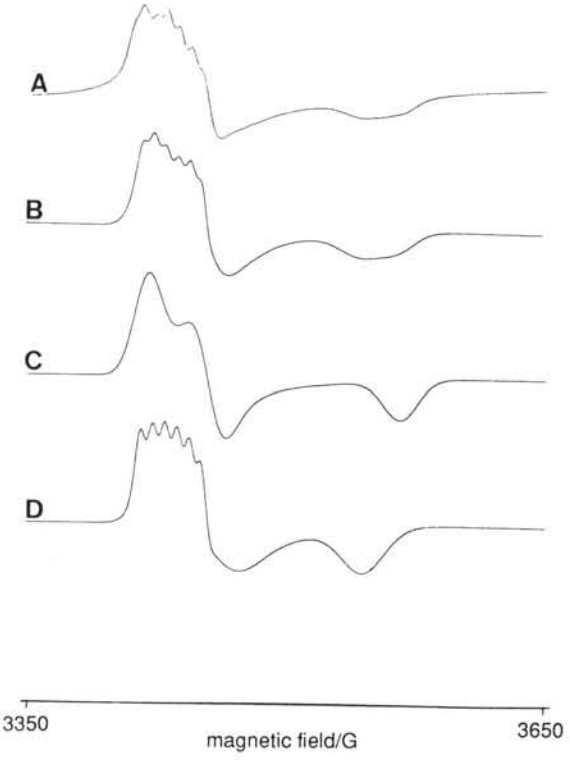

Fig. 4 X-Band EPR spectrum of calcined Cr/mordenite (A), the simulated spectra of species C (C) and D (D) and the sum simulated spectra (B)

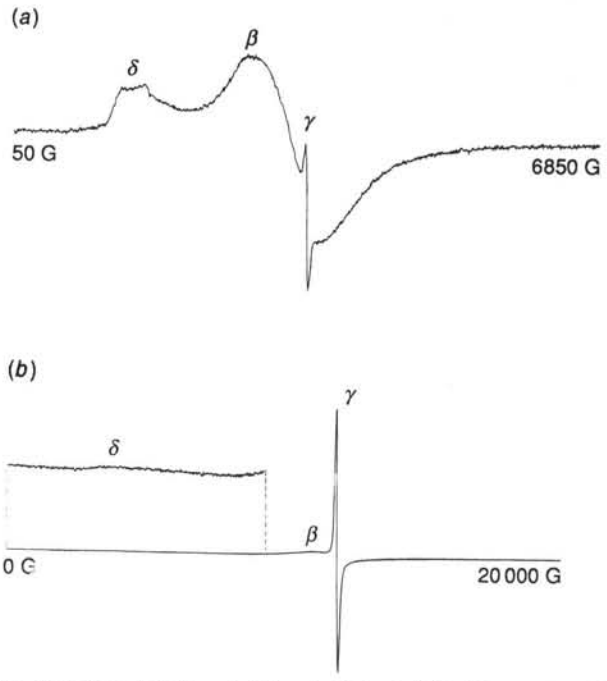

Fig. 5 Experimental X-band (A) and Q-band (B) EPR spectra of supported Cr catalysts (reduced and recalcined 0.2 wt.% Cr/Al_2O_3 catalyst)

Cr^{3+} signals

The X- and Q-band EPR spectra of calcined and reduced Cr/Al_2O_3 catalysts are given in Fig. 5 and 6. The three signals, present in the X-band spectrum, are usually denoted as γ, β

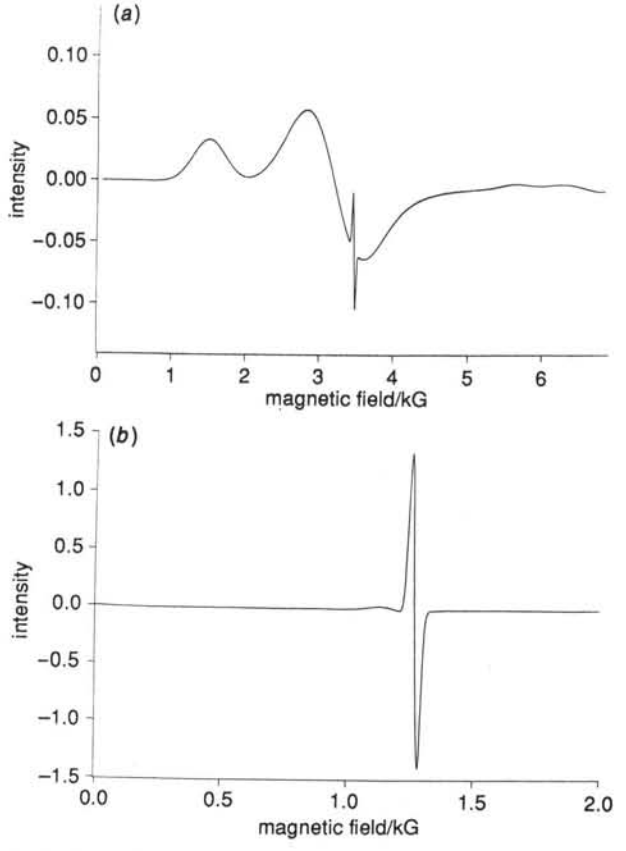

Fig. 6 Theoretical X-band (*a*) and Q-band (*b*) EPR spectra of supported Cr catalysts (reduced and recalcined 0.2 wt.% Cr/Al_2O_3 catalyst)

Table 3 EPR parameters for Cr^{3+} in various inorganic oxides obtained from fitting the experimental powder spectra

material	signal	g_{xx}	g_{yy}	g_{zz}	w_{xx}/G	w_{yy}/G	w_{zz}/G	D/cm^{-1}	E/cm^{-1}
Cr/Al_2O_3	β-signal	2.05	2.05	2.05	740	740	740	0.000	0.000
	δ-signal	1.970	1.565	1.565	800	400	400	0.490	0.163
$Cr/SiO_2 \cdot Al_2O_3$	δ-signal	1.970	1.570	1.570	800	400	400	0.490	0.163
Cr/SiO_2	δ-signal	1.970	1.725	1.725	800	400	400	0.490	0.163
CrAPO-5	C	1.987	1.987	1.987	556	556	556	0.000	0.000
	D	1.987	1.865	1.865	800	400	400	0.490	0.163

and δ. These signals are also observable in the Q-band spectra, although the δ- and β-signals are very weak. The δ- and β-signals can be simulated by using appropriate simulation parameters, which are summarized in Table 3. The obtained values for the zero field parameters, D and E, were obtained by careful inspection of the g *vs.* D or g *vs.* the ratio D/E plots of Fig. 7. These plots were theoretically generated with the simulation programs by using the following parameters: frequency, $f = 9.580$ GHz; spin, $S = 3/2$; step angle, $d\theta = 0.1$; linewidths, $w_x = w_y = w_z = 10$ G and theoretical g-values, $g_x = g_y = g_z = 1.970$.

The β-signal is best fitted by using D and E equal to zero, while simulation of the δ-signal requires the use of high values of D and E($D = 0.490$ cm^{-1} and $E = 0.163$ cm^{-1}). The differences in positions of the δ-signal for Cr/Al_2O_3, Cr/SiO_2 and $Cr/SiO_2 \cdot Al_2O_3$ catalysts can be simulated by introducing small variations in the theoretical g-values. Because the Cr ions are located at the surface, they are subject to large and non-uniform distortions from octahedral/tetrahedral symmetry and consequently the spectra cover several thousand Gauss. Therefore, we have superimposed relatively large linewidths on each resonance. An example of simulated spectra of the β- and δ-signal is given in Fig. 8. The β-signal is a broad isotropic signal with g-values near 2. The δ-signal is characterized by a positive absorption around $g = 4.3$, together with a weaker isotropic signal *ca.* $g = 2$. The signals at lower g-values are due to some simulation noise and are the result of the use of a relatively high $d\theta$-value in the simulation procedure.

By appropriate summation of the individually simulated γ-, δ- and β-signal, the X- and Q-band spectra of Fig. 5 can be reconstructed. This is shown in Fig. 6, and the simulated spectra fit the experimental ones. Such an approach is new and gives strong support for the proposed EPR parameters. The same procedure can be done for the spectra of Cr/SiO_2 and $Cr/SiO_2 \cdot Al_2O_3$ catalysts and there are only minor differences in the exact position of the δ-signal and the relative ratio of the intensities of the different signals. The shape of the experimental δ-signal, however, cannot be exactly obtained by spectrum simulation, not even by the summation of a set of δ-signals with slightly different EPR parameters.

The X- and Q-band EPR spectra of as-synthesized CrAPO-5 molecular sieves are shown in Fig. 9. The X-band spectrum is built up by two signals, a broad signal with g *ca.*

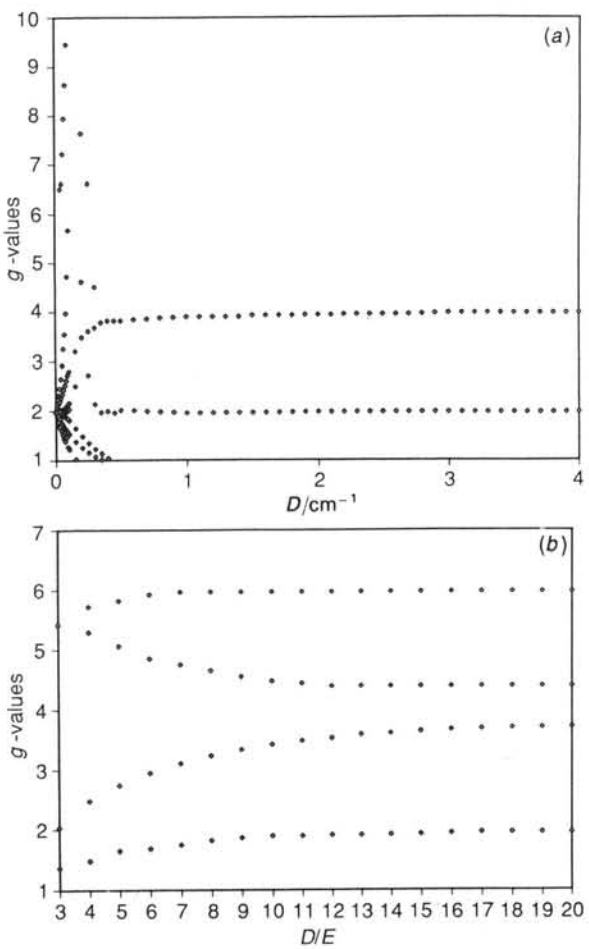

Fig. 7 Theoretical values of the effective g-factors as a function of the zero field parameter D (*a*) and the ratio $D : E$(*b*)

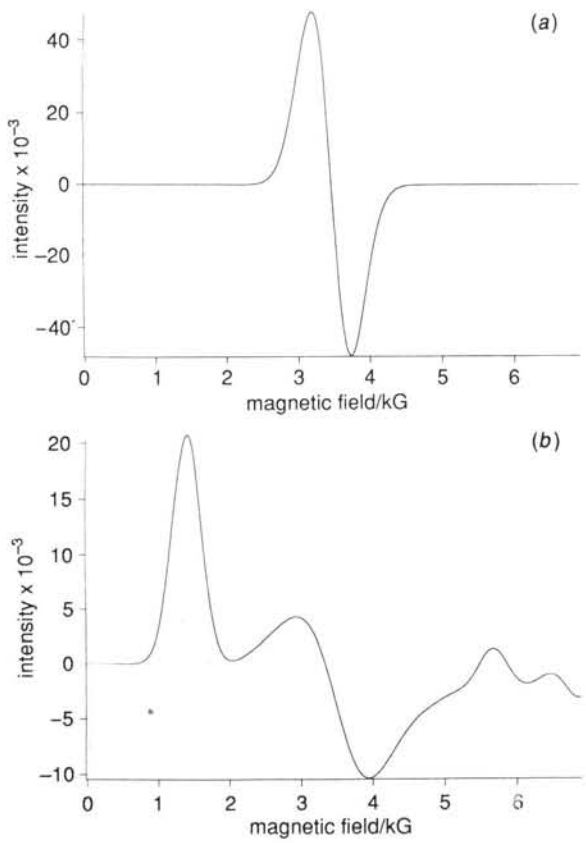

Fig. 8 Theoretical X-band spectrum of the β-signal (*a*) and δ-signal (*b*)

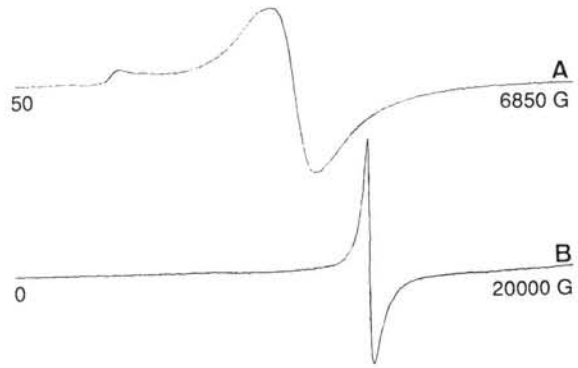

Fig. 9 EPR spectra of CrAPO-5 molecular sieves at 300 K: (A) X-band spectrum and (B) Q-band spectrum

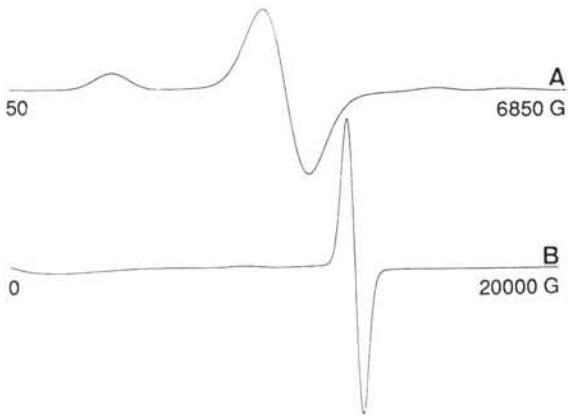

Fig. 10 Simulated EPR spectra of CrAPO-5 molecular sieves: (A) X-band spectrum and (B) Q-band spectrum

2.0 (species C) and a signal with a positive absorption around $g = 4.3$ (species D). The corresponding Q-band EPR spectrum is characterized by an intense signal *ca.* $g = 2.0$. The same analysis can be applied as discussed above and the EPR-parameters of signals C and D, obtained by spectrum simulation, are summarized in Table 3. The corresponding simulated spectra are given in Fig. 10 and there is an excellent agreement between the experimental and the simulated X- and Q-band EPR-spectra. It is also remarkable to see that almost the same simulation parameters, used for simulating the ESR spectra of supported Cr catalysts, can be used to simulate the EPR spectra of the CrAPO-5 molecular sieves.

Discussion

The extensive use of simulation procedures enable us to gather in this paper for the first time detailed parameters from the complex and overlapping EPR spectra of heterogeneous Cr catalysts. The obtained parameters, arising from specific coordination geometries of Cr^{3+} and Cr^{5+} ions in inorganic oxides, are somewhat similar for the different supports. These observations merit a more detailed discussion, which will cover the assignment and the possible coordination environments of the different signals.

Coordination environments of EPR active Cr^{5+}

The axial/rhombic form of the EPR signals of Cr^{5+} indicates an anisotropy of the g factor. In other words, Cr^{5+} is located in a crystalline field whose symmetry is lower than octahedral or tetrahedral. In addition, the EPR signals are quenched in the presence of molecular oxygen owing to dipole–dipole interactions. This observation is indicative for surface Cr^{5+} species. Furthermore, the SQUID measurements proof the mononuclear character of these surface species.

The assignment of the different Cr^{5+} signals can be carried out by comparison with EPR parameters of Cr^{5+} compounds with known structure. The g-values of some Cr^{5+} reference compounds are given in Table 4. On this basis, we can conclude that Cr^{5+} on alumina and silica–alumina is square pyramidal coordinated, whereas Cr^{5+} on silica on mordenite are present in distorted tetrahedal coordination. The exact symmetry of the latter species must be C_{2v} or lower (*e.g.* C_s).

The (pseudo-) tetrahedral coordination of Cr^{5+} may be due to the replacement of Si^{4+} by Cr^{5+} in the oxygen tetrahedra of the silicagel or mordenite framework. In the case of mordenite, aluminium is in close proximity as evidenced by the superhyperfine splitting. Cr^{5+} on alumina occupies octahedral defects giving rise to a square pyramidal coordination. Cr^{5+} on silica–alumina has similar g-values as on alumina, suggesting that this ion is located in the alumina regions of the silica–alumina support. In other words, Cr^{5+} ions have a strong preference for alumina. Additional evidence for this strong interaction is the unresolved superhyperfine splitting of aluminium in the EPR spectra of Cr/Al_2O_3.

Coordination environments of EPR active Cr^{3+}

Two different EPR signals of Cr^{3+} ions are present in amorphous and crystalline inorganic oxides : a broad signal with g *ca.* 2 and zero field parameters D and E equal to 0 cm^{-1} and a signal with a positive lobe in the region $g = 3.5$–5.5 with D and E equal to 0.490 and 0.163 cm^{-1}, respectively.

The isotropic signal of Cr^{3+} with g *ca.* 2 is well documented in the literature and due to Cr^{3+} in nearly octahedral coordination, either in a hexa-aquo complex or clustered form.[20] The other signal has rather unusual EPR parameters and, consequently, comparison with model compounds is difficult. However, in this work we were able to put for the first time numbers on the zero field parameters D and E of the δ-signal, which must be due to a surface Cr species. Indeed, the large anisotropy for the δ-signal of Cr^{3+}, in comparison with bulk Cr^{3+} (*e.g.* Cr^{3+} in Al_2O_3 as ruby with $g_{\|} = 1.984$ and $g_{\perp} = 1.9867$ and $D = 0.193$ cm^{-1} and $E = 0$ cm^{-1} [27]) is indicative of a very distorted Cr^{3+} site. Additional evidence for this conclusion comes from the Q-band spectra, which are always rather weak. This weakness is due to g- and/or D-strain, which may cause broadening of the signals. This is more severe at higher microwave frequencies and such coordinations are therefore much more compatible with surface than with bulk sites. The same reasoning holds for the D signal of CrAPO-5 molecular sieves and means that the EPR active Cr^{3+} in

Table 4 EPR parameters of some Cr^{5+} compounds with known local structure[25,26]

Cr^{5+} compound	g_{xx}	g_{yy}	g_{zz}	local structure
K_2CrOCl_5	1.977	1.977	2.008	square planar
K_2CrOF_5	1.968	1.968	1.959	square planar
Cr^{5+} in Li_3AsO_4	1.9383	1.9383	1.9734	distorted tetrahedral (C_s)
Cr^{5+} in $Ba_5(PO_4)_3Cl$	1.9222	1.9318	1.9737	distorted tetrahedral (C_s)

CrAPO-5 molecular sieves cannot be assigned to isomorphously substituted Cr^{3+}. This conclusion resolves a debate in the literature about the possibility to incorporate Cr^{3+} in the framework of molecular sieves.[28–33]

Conclusions

Spin-Hamiltonian operators for each of the EPR $Cr^{3+/5+}$ resonance signals were proposed and discussed in this paper. A comparative analysis shows that the nature of Cr^{5+} and Cr^{3+} species in heterogeneous catalysts is, on the whole, somewhat similar, independently of the synthesis method and the type of inorganic oxide. This comparative analysis was made possible by the extensive use of spectrum simulations and by measuring EPR spectra both in X- and Q-band. Mononuclear Cr^{5+} ions are axial on alumina and silica–alumina, and rhombic on silica and mordenite. Two different types of Cr^{3+} ions are observed on inorganic surfaces : clustered Cr^{3+} or octahedral Cr^{3+} complexes, both characterized by zero field parameters D and E almost equal to 0 and a strongly distorted Cr^{3+} complex with large values of D and E. On that basis we conclude that CrAPO-5 molecular sieves do not contain isomorphously substituted Cr^{3+}.

B.M.W. acknowledges the National Fund for Scientific Research (N.F.W.O.) for a grant as research assistant and for a travel grant to visit the Chemistry Department of the University of Manchester. This work was financially supported by the Geconcerteerde Onderzoeksaktie of the Flemisch Government and by the Fonds voor Kollectief Fundamenteel Onderzoek (FKFO) under grant No. 2.0050.93. D.C. thanks the Royal Society for financial support. The authors thank Prof. Y. Bruynseraede and Dr. V. Metlushko of the Catholic University of Leuven for the SQUID measurements.

References

1 J. P. Hogan, *Applied Industustrial Catalysis*, Academic Press, vol. 1, New York, 1983, p. 149.
2 M. P. McDaniel, *Adv. Catal.* 1985, **33**, 47.
3 D. E. O'Reilly and D. S. MacIver, *J. Phys. Chem.* 1962, **66**, 276.
4 L. L. Van Rijen and P. Cossee, *Discuss. Faraday Soc.* 1966, **41**, 277.
5 D. Cordischi, V. Indovina and M. Occhiuzzi, *Appl. Surf. Sci.*, 1992, 55, 233.
6 C. Groeneveld, P. P. M. M. Wittgen, P. L. M. Van Kersbergen, L. M. Mestrom, C. E. Nuijten and G. C. A. Schuit, *J. Catal.*, 1979, **59**, 153.
7 V. B. Kazanski and J. Turkevich, *J. Catal.*, 1967, **8**, 231.
8 D. D. Beck and J. H. Lunsford, *J. Catal.*, 1981, **68**, 121.
9 J. F. Hemidy, F. Delavennat and D. Cornet, *J. Chim. Phys.*, 1973, **11–12**, 1716.
10 J. F. Hemidy and D. Cornet, *J. Chim. Phys.*, 1974, **5**, 739.
11 M. Huang, Z. Deng and Q. Wang, *Zeolites*, 1990, **10**, 272.
12 D. Cordischi, M. C. Campa, V. Indovina and M. Occhiuzzi, *J. Chem. Soc., Faraday Trans.*, 1994, **90**, 207.
13 B. M. Weckhuysen, L. M. De Ridder, P. J. Grobet and R. A. Schoonheydt, *J. Phys. Chem.*, 1995, **99**, 320.
14 B. M. Weckhuysen, L. M. De Ridder and R. A. Schoonheydt, *J. Phys. Chem.* 1993, **97**, 4756.
15 B. M. Weckhuysen, A. A. Verberckmoes, A. L. Buttiens and R. A. Schoonheydt, *J. Phys. Chem.*, 1994, **98**, 579.
16 B. M. Weckhuysen, I. E. Wachs and R. A. Schoonheydt, *Stud. Surf. Sci. Catal.*, 1995, **91**, 151.
17 B. M. Weckhuysen and R. A. Schoonheydt, *Zeolites*, 1994, **14**, 360.
18 B. M. Weckhuysen, H. J. Spooren and R. A. Schoonheydt, *Zeolites*, 1994, **14**, 450.
19 B. M. Weckhuysen and R. A. Schoonheydt, *Stud. Surf. Sci. Catal.*, 1994, **84**, 965.
20 D. Collison and F. E. Mabbs, *J. Chem. Soc. Dalton Trans.*, 1982, 1565.
21 F. E. Mabbs and D. Collison, *Electron paramagnetic resonance of d transition metal compounds*, Elsevier Science, Amsterdam, 1992.
22 A. Ellison, *J. Chem. Soc., Faraday Trans. 1*, 1984, **80**, 2581.
23 R. Spitz, *J. Catal.*, 1974, **35**, 345.
24 A. Cimino, D. Cordishi, S. De Rossi, G. Ferraris, D. Gazzoli, V. Indovina, M. Occhiuzzi and M. Valigi, *J. Catal.*, 1991, **127**, 761.
25 M. Greenblatt, *J. Chem. Educ.*, 1980, **57**, 546.
26 K. Nag and S. N. Bose, *Struct. Bonding (Berlin)*,1985, **63**, 153.
27 D. E. O'Reilly and D. S. MacIver, *J. Phys. Chem.* 1962, **66**, 276.
28 N. Rajic, D. Stojakovic, S. Hocevar and V. Kaucic, *Zeolites*, 1993, **13**, 384.
29 J. D. Chen, J. Dakka, E. Neeleman and R. A. Sheldon, *J. Chem. Soc., Chem. Commun.*, 1993, 1379.
30 D. Demüth, K. K. Unger, F. Schüth, V. I. Srdanov and G. D. Stucky, *J. Phys. Chem.*, 1995, **99**, 479.
31 J. D. Chen and R. A. Sheldon, *J. Catal.*, 1995, **153**, 1.
32 O. Nakumura, J. S. Mambrim, H. O. Pastore, E. J. S. Vichi, F. G. Gandra, E. C. Silva, H. Vargas and J. Pelzi, *J. Chem. Soc., Faraday Trans.*, 1992, **88**, 2071.
33 N. Van der Puil, J. C. Jansen, Widyawatti and H. van Bekkum, *Stud. Surf. Sci. Catal.*, 1994, **84**, 211.

Paper 6/00203J; *Received* 10*th January*, 1996